2025, 10 (44s) e-ISSN:2468-4376 https://jisem-journal.com/

Multi-Plant Leaf Disease Identification Using Vein-Related Symptom Analysis

Preeti Yadav¹, Parvinder Singh²

preeti.schcse@dcrustm.org¹
parvindersingh.cse@dcrustm.org²

DCRUST Murthal, Haryana, India, Pin code 131027

DCRUST Murthal, Haryana, India, Pin code 131027

ARTICLE INFO

ABSTRACT

Received: 20 Oct, 2024 Revised: 18 Nov, 2024

Accepted: 15 Dec, 2024

A promising solution to enhance yield efficiency is Plant Leaf Disease Detection (PLDD). Nevertheless, none of the traditional frameworks focused on the vein-related symptoms during PLDD. Therefore, this paper proposes a robust MER-DS-EfficientNet and EZWS-based vein-related symptom analysis and multi-PLDD. Initially, the plant Leaf Disease (LD) datasets are collected and then pre-processed. Then, the background region is eliminated, followed by density heat map generation. Afterward, the feature extraction and feature reduction are done. Here, to identify the type of plant leaf, the proposed MER-DS-EfficientNet is utilized. Then, to recognize the healthy and disease-affected leaves, the Color Component Analysis (CCA) is done. Next, the disease region is segmented, followed by feature extraction and feature reduction. Also, via the hessian matrix, the Vein Region (VR) is fragmented. Then, from the vein factors, the VER is computed. Lastly, the proposed MER-DS-EfficientNet significantly classifies the multi-plant LDs. The proposed method performed better, with 98.9942% accuracy. ac tincidunt vitae semper.

Keywords: Plant Leave Disease Detection (PLDD), Major Field Crops (MFC), Vein-related Symptom (VS), Vein Elongation Ratio (VER), Maximal Entropy Regularized-Double Sigmoidweighted EfficientNet (MER-DS-EfficientNet), Exponential Zettl Watershed Segmentation (EZWS), and Deep Learning (DL)

1. INTRODUCTION

A prime role is played by agriculture in the advancement of developing countries (Singh et al., 2023). Hence, the staple factors of foods are crops like rice, wheat, maize, and sorghum (Jwar) (Khan et al., 2022) (Gonzalez et al., 2024). Nevertheless, the crop's growth is mainly affected by plant diseases like pest diseases and gray leaf spots (Li et al., 2022) (Bi et al., 2023). Timely prediction of Plant Leaf Diseases (PLDs) significantly upgrades the production quality (Jiang et al., 2022). To perform PLD detection, previous studies implemented a Deep Learning (DL) approach (Alharbi et al., 2023) (Latif et al., 2022).

To detect the multiple diseases in crops like rice and wheat, the existing models utilized various kinds of Convolutional Neural Network (CNN), including DenseNet21 and MobileNetV2 (Kundu et al., 2022) (Ahad et al., 2023). Nevertheless, none of the existing studies concentrated on the VS, thus hiding the early clues about the diseased plants. Thus, a robust MER-DS-EfficientNet and EZWS-based vein-related symptom analysis and multi-PLDD are proposed in this paper.

Problem Statement

The drawbacks of the prevailing studies are listed further,

None of the conventional works focused on VS, thus obscuring the early indicators of plant diseases.

2025, 10 (44s) e-ISSN:2468-4376 https://jisem-journal.com/

- The prevailing (Masood et al., 2023) struggled to differentiate the maize and sorghum owing to their similar structure.
- In the existing (Joseph et al., 2024), the presence of noisy appearance affected the model's outcomes.
- The traditional (Tanveer et al., 2024) failed to differentiate the mature leaf yellowing and diseases like rust.
- Some of the conventional frameworks had high computational complexity owing to the massive amount of feature size.

2. OBJECTIVES

The research work's major goals are given below,

- The proposed work considers vein-related symptoms like VER to improve the model's performance.
- The Density Heat Map (DHM) generation is done to capture the subtle difference between maize and sorghum leaves.
- A novel Non-Local Means Log Chicharro Denoising (NLMLCD) is employed to perform noise reduction.
- Here, a CCA is done to differentiate the aged and disease-affected leaves.
- An effective Principal Differential Group Component Analysis (PDGCA) is introduced to reduce the feature dimensions.

The paper is structured as: the related frameworks are demonstrated in Section 2; the proposed scheme is showcased in Section 3; the proposed model's performance is validated in Section 4; the article is concluded in Section 5.

3. LITERATURE REVIEW

(Tanveer et al., 2024) scrutinized a transfer learning-based maize crop LD detection. Here, to classify the features into healthy and infected crops, the Visual Geometry group and Gaussian Naïve Bayes (VG-GNBNet) were introduced. This work had high robustness. Nevertheless, this model didn't concentrate on differentiating the mature leaf yellowing and diseases.

(Masood et al., 2023) offered a DL-based effective maize PLD recognition using MaizeNet. For classifying the various maize crop leaf disorders, the faster Region Convolutional Neural Network (RCNN) was presented. This model had better outcomes. However, this model was less effective owing to the low inter-class variance.

(Jiang et al., 2021) applied a rice and wheat LD classification using multi-task deep transfer learning. Here, to classify both the rice and wheat leaves into healthy and diseased, an improved VGG16 model was developed. This framework had high adaptability. Yet, this model had vanishing gradient issues.

(Joseph et al., 2024) recognized real-time plant disease detection based on DL approaches. Here, to detect plant diseases, eight fine-tuned DL models, including Xception and MobileNet were introduced. The developed model had higher supremacy. Nevertheless, the presence of noise affected the detection results.

(Ma et al., 2023) examined a maize LD recognition model using YOLOv5 along with an attention mechanism. For identifying the maize LDs like gray spots and rust, the YOLOv5 with CA was used. Here, the Coordinate Attention (CA) mechanism helped to upgrade the model's performance. Nevertheless, this framework was only proved with the limited number of classes.

4. METHODS

This work implemented an effective MER-DS-EfficientNet and EZWS-based VS analysis and multi-PLDD model. In Figure 1, the proposed work's architecture is given.

2025, 10 (44s) e-ISSN:2468-4376 https://jisem-journal.com/

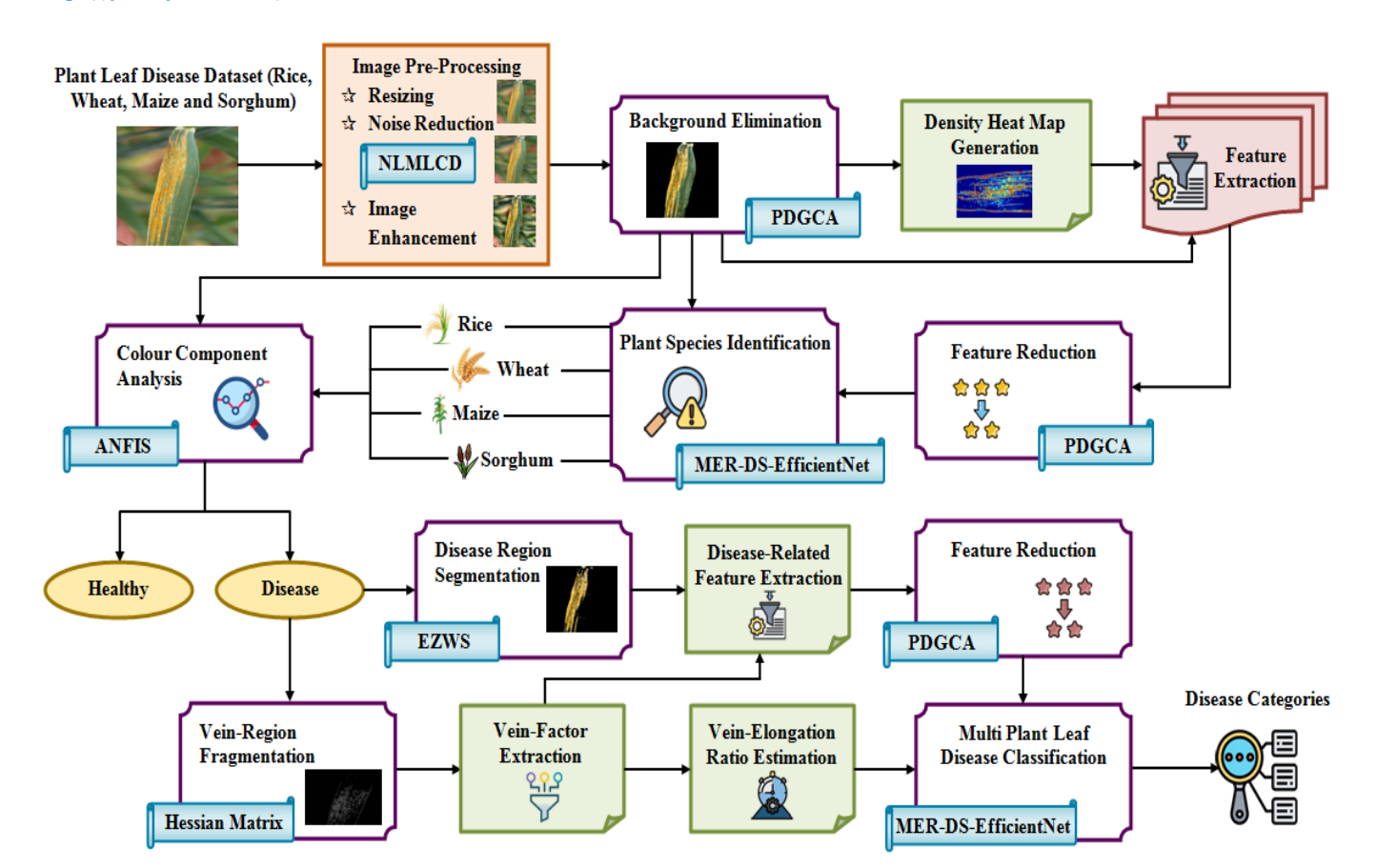


Figure 1: The proposed model's framework

Plant Leaf Disease Dataset

Primarily, the PLD datasets are collected for rice, wheat, maize, and sorghum.

$$\mathcal{O}_u = \langle \mathcal{O}_1, \mathcal{O}_2, \dots, \mathcal{O}_U \rangle$$
 Here, $u = 1 to U$ (1)

Here, U specifies the number of collected input plant leaf images Θ_u .

Image Pre-Processing

Chicharro Technique (LCT) is used.

Then, to upgrade the classification efficiency, Θ_u is pre-processed. The original proportionalities of all the images are transformed into the same dimensions in resizing. Next, the resized images (\mathfrak{R}_u) are subjected to the NLMLCD. The Non-Local Means Denoising (NLMD) effectively removes the random noises without losing image details. Nevertheless, the NLMD is sensitive to the choice of window size. Thus, to assume the window size (Ξ) , the Log Chickenge Tackering (LCM) is a sensitive to the choice of window size.

$$\Xi(\mathfrak{R}_u) = \sum_{u=1}^{U} \left(\mathfrak{R}_u^4 - 16\mathfrak{R}_u^2 + 5\mathfrak{R}_u \right)$$
(2)

2025, 10 (44s) e-ISSN:2468-4376 https://jisem-journal.com/

$$\partial(px) = \frac{\sum_{\lambda \in \Xi} \varpi(px, \lambda) \Re_u(\lambda)}{\sum_{\lambda \in \Xi} \varpi(px, \lambda)}$$
(3)

Here, $\partial(px)$ specifies the denoised image, (px,λ) signifies the intensity pixels, and ϖ portrays the weight value. Finally, during the image enhancement, the low level resolutions of the images $\partial(px)$ are enhanced into high level resolutions. Therefore, the pre-processed images are mentioned as (φ_{∇}) .

Background Elimination

Next, by using the proposed PDGCA, the background of φ_{∇} is eliminated. The Principal Component Analysis (PCA) had global pattern recognition and robustness. Yet, the PCA had considerable computational time. So, to approximate the eigenvalue, the proposed method employs the Differential Group Transform (DGT). At first, φ_{∇} is represented as an input matrix (\aleph) , which has the flattened (pixel) version of the images. Then, the \aleph is standardized as below,

$$\delta^{\circ} = \frac{\aleph - \upsilon}{\eta} \tag{4}$$

Where, δ° specifies the standardized data, υ and η signify the mean and standard deviation, respectively. Next, to showcase the relationship among the pixel values, the covariance matrix $(\Omega)_{is}$ generated.

$$\Omega = \frac{1}{Z - 1} \left(\delta^{\circ T}, \delta^{\circ} \right), \qquad z = 1 \text{ to } Z$$
(5)

Here, z = 1 to Z portrays the total number of pixel values. Then, the Ω is decomposed into eigenvectors (λ) and eigenvalues (ℓ) .

$$\Omega \cdot \hat{\lambda} = \ell \cdot \hat{\lambda} \tag{6}$$

Here, by using the DGT (αx) , the eigenvalue is approximated.

$$\alpha x(\ell) = \sum_{z=1}^{Z} \left(\ell - \frac{1}{2}\right)^{2} \tag{7}$$

So, according to the $\alpha x(\ell)$, the $\dot{\lambda}$ is sorted in descending order. Next, the eigenvector with the highest eigenvalue is considered as the dominant component $(\partial^{\circ}\mu)$. The dominant parts are assumed as the background region. The background is eliminated based on $\partial^{\circ}\mu$. Therefore, the Background Eliminated Image (BEI) is illustrated as $(\beta\Phi)$.

2025, 10 (44s) e-ISSN:2468-4376 https://jisem-journal.com/

The PDGCA's pseudo-code is given below,

Input: Pre-processed image φ_{∇}

Output:BEI $\beta\Phi$

Begin

Initialize $^{\aleph}$, $^{\lambda}$, $^{\Omega}$ and $^{\varphi_{\nabla}}$

For 1 to each φ_{∇} do,

Generate input matrix (\aleph)

$$\delta^{\circ} = \frac{\aleph - \upsilon}{\eta}$$

Standardize

Create covariance matrix

$$\Omega = \frac{1}{Z - 1} \left(\delta^{\circ T}, \delta^{\circ} \right)$$

Calculate eigenvalue and eigenvector

$$\Omega \cdot \mathbf{\hat{\lambda}} = \ell \cdot \mathbf{\hat{\lambda}}$$

 $\mathbf{Apply}\,\mathrm{DGT}\big(\!\alpha\!x\big)$

Identify dominant components

Eliminate background region

End For

 $_{\text{End}}^{\text{Return }\beta\Phi}$

Density heat map generation

The DHM $(D\infty)$ is generated from $\beta\Phi$ to showcase the distribution of the intensities according to their density. The DHM helps to visualize the hidden patterns and subtle variations and differentiates the species with similar structures.

Feature extraction

From $^{\beta\Phi}$, crucial features like shape, texture, color, and variance are extracted. Similarly, from $^{D\infty}$, the density features like density peaks, density valleys, and gradients are extracted. Therefore, the extracted features are mentioned as (γ_{Ω}) .

Feature reduction

By using the proposed PDGCA, the dimensions of γ_{Ω} are reduced while preserving the significant details. The proposed PDGCA is explained in Section 3.3.

2025, 10 (44s) e-ISSN:2468-4376 https://jisem-journal.com/

$$\Lambda_{y} = \|\Lambda_{1}, \Lambda_{2}, \dots, \Lambda_{Y}\|_{\text{Where, }} y = 1, 2, \dots Y$$
(8)

Where, Y represents the number of reduced features (Λ_y) .

Plant species identification

Afterward, $^{\Lambda_y}$ and $^{\beta\Phi}$ are inputted into the proposed MER-DS-EfficientNet, which classifies the types of plant leaf. Owing to the compound scaling, the EfficientNet had high computational efficiency. Still, it had overfitting issues and poor learning efficiency. Therefore, the proposed method introduces the Maximal Entropy Regularization (MER) and Double Sigmoid-weighted Linear Unit (DSiLU) activation. In Figure 2, the proposed MER-DS-EfficientNet's architecture is presented.

Maximum Entropy Regularization

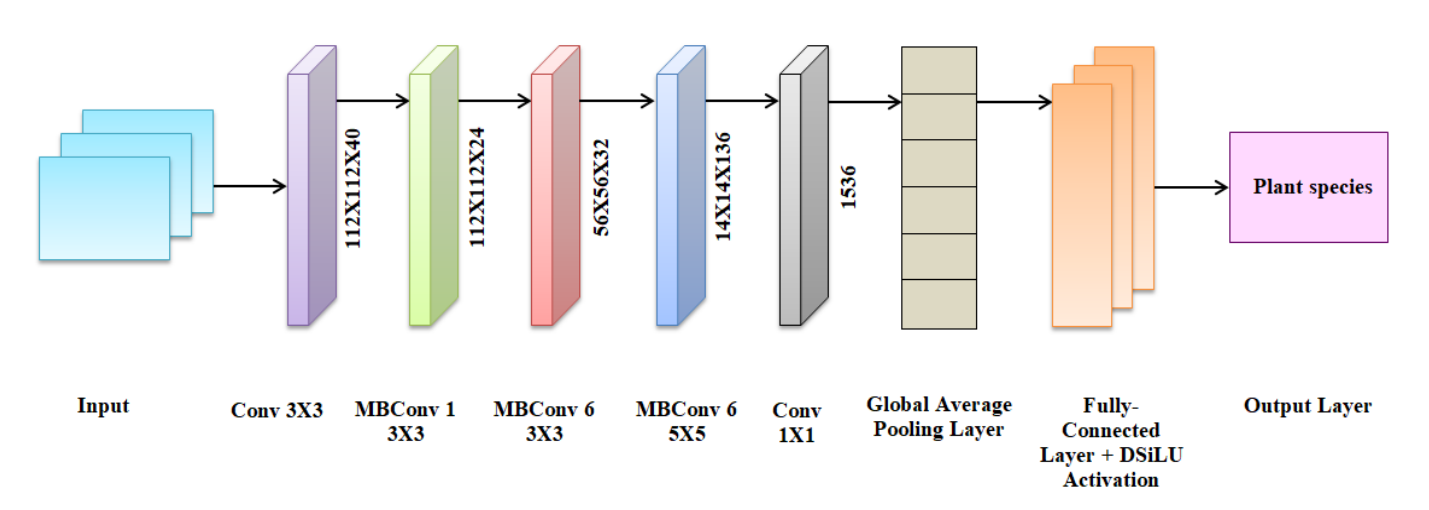


Figure 2: The MER-DS-EfficientNet's structure

The EfficientNet introduces a compound scaling $(X_{scale})_{method}$ that increases the depth $(\partial p)_{, width}$ $(\omega d^{\Psi})_{, and}$ resolution $(Rs^{\Psi})_{of}$ the network via compound coefficient $(\Psi)_{, and}$.

$$X_{scale} = \langle \hat{o}p^{\Psi}, \omega d^{\Psi}, Rs^{\Psi} \rangle$$
(9)

Initially, the inputs, such as reduced features and background-eliminated images are fed into the convolutional layer, where the feature map (F_{map}) is generated.

Then, via the collection of Mobile inverted Bottleneck convolutional layer (MBConv), the feature map is processed with various configurations. To capture rich spatial information, the MBConv uses depth-wise separable convolution and **1x1 point-wise convolution**. Furthermore, to capture important features, the MBConv establishes the Squeeze-and-Excitation (SE) layers.

Also, the 1x1 convolution is employed to increase the number of channels, attaining relevant features.

Then, the global average pooling operation is applied to reduce the feature dimensions.

2025, 10 (44s) e-ISSN:2468-4376 https://jisem-journal.com/

The fully-connected layer is used to classify the different types of PLD regarding the reduced feature map (κ) .

$$Z_{ful}(\kappa) = I_{DSiLU} \times (\kappa \cdot \mathfrak{I}_{wit} + O_{bias})$$
(10)

Where, O_{bias} portrays the bias.

To upgrade the learning efficiency, the DSiLU activation $(I_{DSiLU})_{is}$ used.

$$I_{DSiLU}(\kappa) = \kappa \cdot \frac{1}{1 + \exp\left(-\kappa * \frac{1}{1 + \exp(-\kappa)}\right)}$$
(11)

Here, by using the MER, the weight values (\mathfrak{I}_{wit}) are initialized, thus reducing the overfitting issues.

$$\mathfrak{I}_{wit} = -\sum \Gamma(\kappa) \log \Gamma(\kappa) \tag{12}$$

The output layer $(Ol)_{\text{displays}}$ the identified plant types like rice $(\mathfrak{R}_{ice})_{\text{, wheat}}(W_{heat})_{\text{, maize}}(M_{aize})_{\text{, and sorghum}}$ (S_{orghum})

$$Ol = \left\{ \Re_{ice}, W_{heat}, M_{aize}, S_{orghum} \right\}$$
(13)

The MER-DS-EfficientNet's pseudo code is presented below,

Input: Λ_y and $\beta\Phi$ Output: Plant species

Begin

Initialize Λ_{y} , $\beta\Phi$, \mathfrak{I}_{wit} , I_{DSiLU} and O_{bias}

For 1 to each input do,

Execute compound scaling

$$X_{scale} = \langle \partial p^{\Psi}, \omega d^{\Psi}, Rs^{\Psi} \rangle$$

Generate feature map $(F_{map})_{via}$ convolution Apply MBConv layers and 1x1 convolutions

#Global average pooling

Reduce feature dimensions Determine fully-connected layer,

$$Z_{ful}(\kappa) = I_{DSiLU} \times (\kappa \cdot \mathfrak{I}_{wit} + O_{bias})$$

Activate DSiLU

Regularize weight $\mathfrak{I}_{wit} = -\sum \Gamma(\kappa) \log \Gamma(\kappa)$ Display output

End For

$$Ol = \left\{ \mathfrak{R}_{ice}, W_{heat}, M_{aize}, S_{orghum} \right\}$$

Return End

2025, 10 (44s) e-ISSN:2468-4376 https://jisem-journal.com/

Also, CCA is done.

3.8 Color component analysis

Here, based on the Adaptive Neuro-Fuzzy Inference System (ANFIS), the BEI of the respected plant leaf is subjected to the CCA. The RGB (r,g,b) values are considered to identify the healthy and disease-affected leaves. Primarily, using the Gaussian membership function (G_{auss}) , the fuzzification is done.

$$G_{auss}(\beta\Phi) = \exp^{-\frac{1}{2}\left(\frac{\beta\Phi - ctr}{wid}\right)^2}$$
(14)

Here, *ctr* and *wid* signify the center and width, respectively.

Next, to identify the healthy and disease-affected plant leaves, the rules (Fuzz) are framed.

$$Fuzz(r,g,b) = \begin{cases} If(r,b \le 100 \& g \ge 120), & healthy \\ If(r,g \ge 100 \& b \le 80), & yellowing \\ If(r \ge 100 \& g \ge 60 \& b \le 50), & brown spots \\ If(r \ge 120 \& g \le 100 \& b \ge 50), & disease \end{cases}$$
(15)

Also, to differentiate mature yellowing and diseases, the Normalized Difference Vegetation Index (NDVI) $(\tau_{ndvi})_{is}$ used.

$$yellowing \rightarrow \begin{cases} If(\tau_{ndvi} = 0.4to0.6), & mature yellow \\ If(\tau_{ndvi} < 0.4), & disease \end{cases}$$
(16)

Similarly, the fuzzy rules are normalized. Contrarily, the fuzzy data is converted into crisp data. Lastly, the summation layer (Sm)helps to conclude the results regarding the preceding layers.

$$Sm = \{Hl, Di\} \tag{17}$$

Here, Hl and Di designate the healthy and diseased leaves, respectively.

Disease region segmentation

Then, by using the proposed EZWS, the disease region is segmented from Di. The Watershed Segmentation (WS) had high versatility and efficiency. Nevertheless, owing to the improper marker selection, it had overlapping regions. The proposed work introduces the Exponential Zettl Scheme (EZS) to select the appropriate marker.

Mostly, the gradient (Δ_{grad}) is computed as below,

$$\Delta_{grad}(\alpha_1, \alpha_2) = \sqrt{(Di)_{\alpha_1} + (Di)_{\alpha_2}}$$
(18)

Here, α_1 and α_2 signify the pixel coordinates. Then, by using the EZS, the marker (Π) is initialized.

2025, 10 (44s) e-ISSN:2468-4376 https://jisem-journal.com/

$$\Pi = \sum_{r=1}^{R} \left(\Delta_{grad}^{4} - 2\Delta_{grad}^{2} + 1 \right)$$
(19)

Where, r = 1 to R demonstrates the maximum iterations. The regional markers are labeled according to the initialized marker. Thus, the distance $(\mu_{Dis})_{is}$ calculated between the labeled regional marker $(L_{reg})_{and}$ the maximum regional marker $(t_{max})_{and}$.

$$\mu_{Dis}(L_{reg}, t_{max}) = \sqrt{\sum_{r=1}^{R} (L_{reg} - t_{max})^2}$$
 (20)

The flooding process is done based on the shortest distance between the pixel values. Next, to locate each pixel, the nearest regional marker is used. Here, to segment the disease-affected region $\binom{D_{reg}}{}$, the located similar pixel values are merged.

Disease-related feature extraction

From D_{reg} , the disease-related features (H^{∞}) like shape, entropy, skewness, energy, and homogeneity are extracted.

Feature reduction

Then, the dimensions of the H^{∞} are reduced by using the proposed PDGCA, which is derived in Section 3.3. The dimensionality-reduced features are shown as (E_{red}) .

Vein region fragmentation

Similarly, the VR from Di is segmented by using the Hessian matrix, which highlights the edges and curves corresponding to the VR. The proposed work improves the efficiency of the MPDD by focusing on the VR of the plant. Here, based on the second partial derivatives (2∂) of the image intensity, the hessian matrix $(X_{hessian})$ is created.

$$X_{hessian}(\phi, \xi) = \begin{bmatrix} 2\partial_{\phi\phi} & 2\partial_{\phi\xi} \\ 2\partial_{\phi\xi} & 2\partial_{\xi\xi} \end{bmatrix}$$
(21)

Here, (ϕ, ξ) signify the spatial coordinates. The hessian matrix is enhanced using the second-derivative Gaussian convolution, which aids in measuring the vesselness. Then, to reveal the direction of intensity change, the eigenvalues (\mathcal{M}) are calculated from the enhanced Hessian matrix $(X_{hessian})$.

$$\gamma \lambda = \frac{2\partial_{\phi\phi} + 2\partial_{\xi\xi} \pm \sqrt{\left(2\partial_{\phi\phi} + 2\partial_{\xi\xi}\right)^2 - 4\left(2\partial_{\phi\phi} 2\partial_{\xi\xi} - 2\partial_{\phi\xi}^2\right)}}{2} \tag{22}$$

2025, 10 (44s) e-ISSN:2468-4376 https://jisem-journal.com/

$$\begin{cases} IF(\gamma\lambda_1 = 0.5to1.5 \& \& \gamma\lambda_2 = 0.05to0.2), & veinregion \\ Else, & non-vein region \end{cases} \tag{23}$$

The larger $^{\gamma\lambda}$ indicates the direction of the intensity change, whereas the smaller $^{\gamma\lambda}$ represents the direction of the vein. Therefore, the segmented VR is mentioned as $(\hbar se)$.

Vein factor extraction

Then, from $\hbar se$, the vein factors $(F_{vein})_{like}$ vein length $(\ell en)_{vein}$, vein area $(\alpha rea)_{vein}$, vein connectivity, and vein density are extracted.

Vein elongation ratio

Also, to reveal early clues about PLD, the vein elongation ratio (vein-related symptom) is estimated.

$$VE_{ratio} = \frac{\ell en}{\alpha rea}$$
 (24)

Here, VE_{ratio} designates the VER.

Multi-plant leaf disease classification

Here, E_{red} , F_{vein} and VE_{ratio} are fed into the proposed MER-DS-EfficientNet, which is derived in Section 3.7. The proposed MER-DS-EfficientNet classifies the PLD like rice (leaf smut, brown spot, as well as bacterial leaf blight), wheat (septoria and stripe rust), maize (common rust, gray leaf spot, and blight), and sorghum (anthracnose and rust).

5. RESULTS

Here, the proposed model's performance is evaluated to demonstrate the model's reliability.

Dataset description

By using four datasets, namely the rice leaf dataset, wheat leaf dataset, maize leaf dataset, and sorghum dataset, the proposed model is implemented. From the whole information, 80% and 20% of images are allocated for training and testing, respectively.

Table 1: Image results

Sample /	Rice	Wheat	Maize	Sorghum
Process	(leaf smut)	(stripe rust)	(gray spot)	(rust)
Input	0 10-9			

2025, 10 (44s) e-ISSN:2468-4376 https://jisem-journal.com/

Resizing	0 10 9		
Noise reduction	0.119		
Contrast enhancement			
Background elimination			
Disease region segmentation			
VR segmentation			

Table 1 exhibits the sample image outcomes of the proposed model.

2025, 10 (44s) e-ISSN:2468-4376 https://jisem-journal.com/

Performance assessment

The performance of the proposed approach is validated by comparing it with existing models.

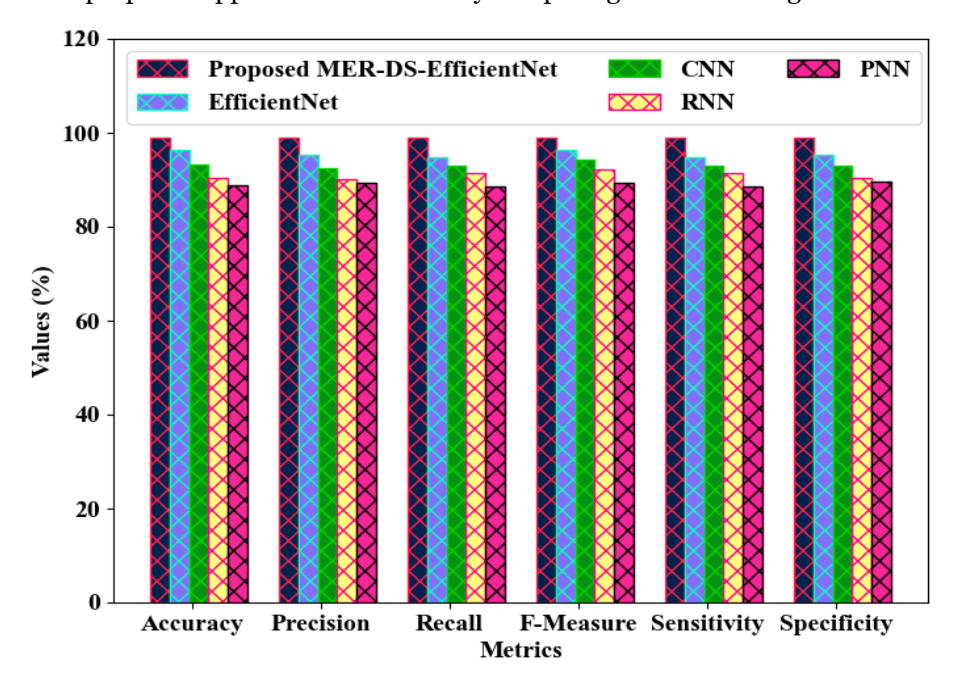


Figure 3: Performance analysis for multi-PLD classification

The proposed MER-DS-EfficientNet's performance is evaluated with the prevailing EfficientNet, CNN, Recurrent Neural Network (RNN), and Probabilistic Neural Network (PNN) in Figure 3. Regarding accuracy, precision, recall, f-measure, sensitivity, and specificity, the proposed MER-DS-EfficientNet obtained 98.9985%, 98.9942%, 98.9975%, 98.9949%, 98.9975%, and 98.9842%, respectively. But, owing to poor regularization, the existing algorithms had limited performance. Due to the presence of DSiLU activation, the proposed algorithm performed well in the PLDD.

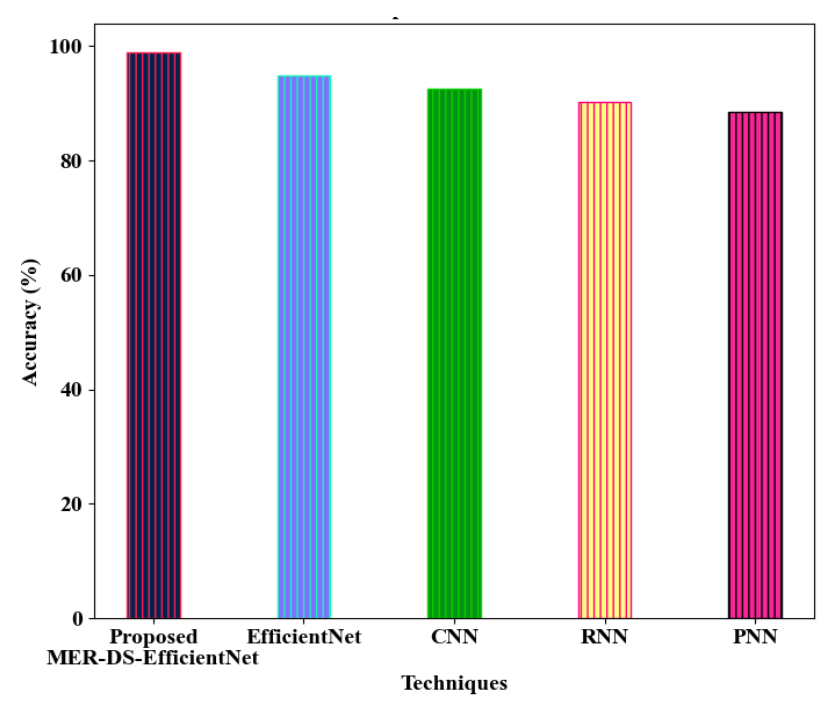


Figure 4: Performance assessment of the MER-DS-EfficientNet

2025, 10 (44s) e-ISSN:2468-4376 https://jisem-journal.com/

In Figure 4, the performance of the proposed MER-DS-EfficientNet and the conventional classifiers is analyzed regarding plant species identification. Regarding accuracy, the MER-DS-EfficientNet attained 98.9953%; while, the traditional EfficientNet obtained 94.9539%. Therefore, the efficiency of the proposed work was proved.

Table 2: Training time

Methods	Training time (ms)
Proposed MER-DS-EfficientNet	59209
EfficientNet	83940
CNN	99201
RNN	114022
PNN	159343

Table 3: Cohen's kappa

Methods	Cohen's kappa
Proposed MER-DS-EfficientNet	0.9875
EfficientNet	0.8532
CNN	0.7425
RNN	0.5316
PNN	0.4789

The comparative analysis of the proposed MER-DS-EfficientNet and the conventional algorithms are represented in Tables 2 and 3. Regarding training time and Cohen's kappa, the MER-DS-EfficientNet obtained 59209ms and 0.9875; while, the traditional PNN attained 159343ms and 0.4789. Thus, the proposed method had low time complexity.

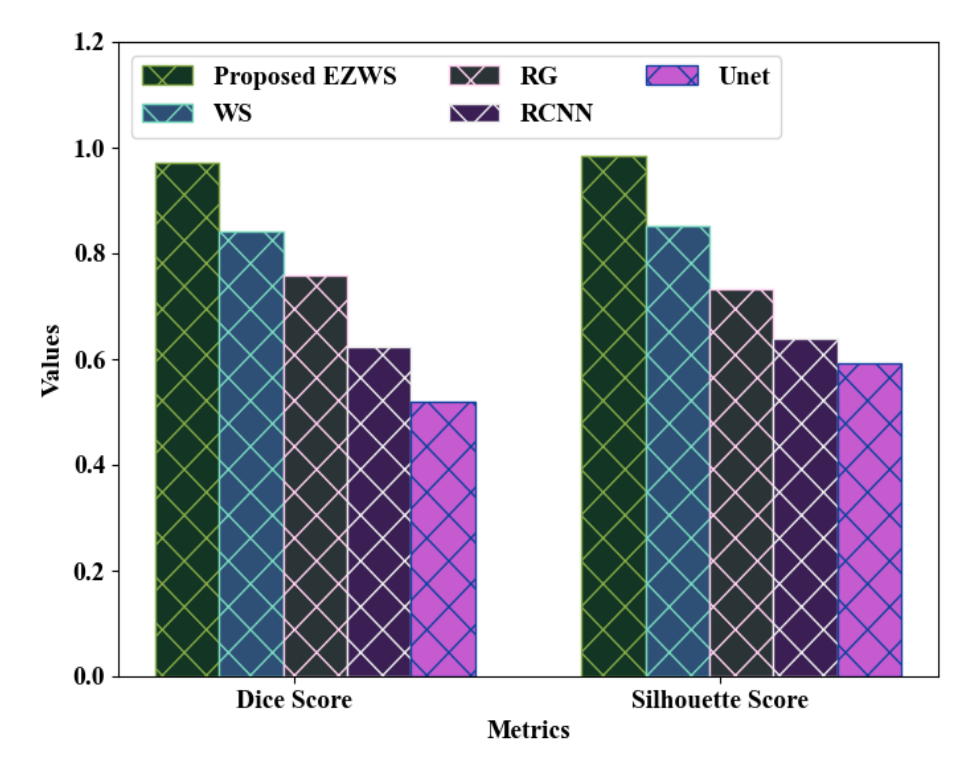


Figure 5: Performance validation of the proposed EZWS

2025, 10 (44s) e-ISSN:2468-4376 https://jisem-journal.com/

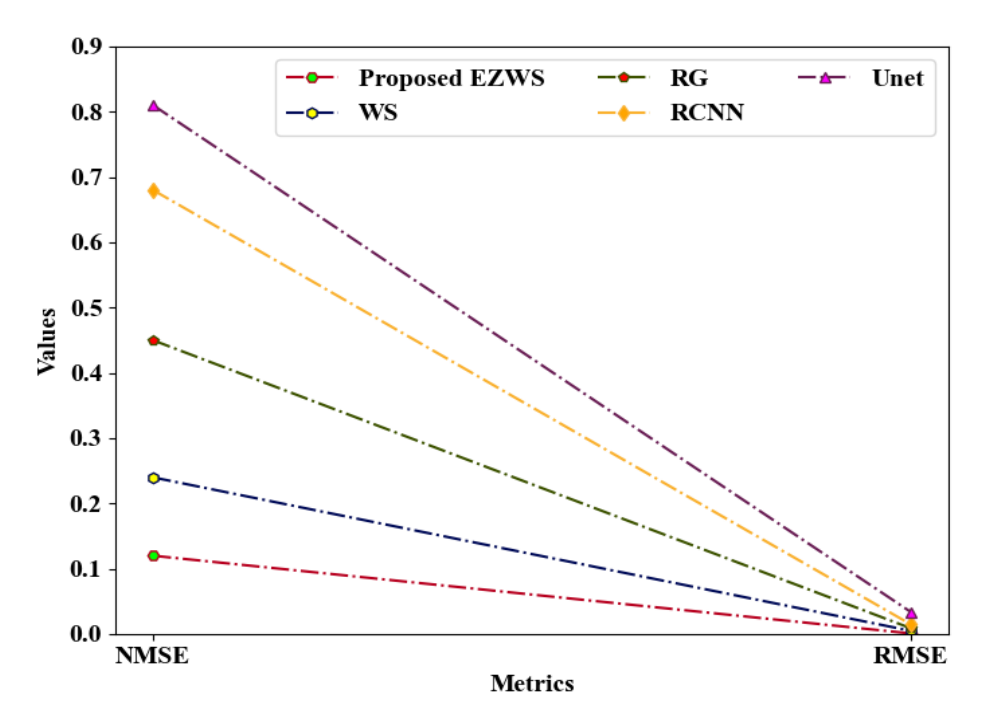


Figure 6: NMSE and RMSE

The presence of EZS helps foraugmenting the segmentation quality. In Figure 5, the performance of the proposed EZWS and the conventional algorithms like WS, Region Growing (RG), Region Convolutional Neural Network (RCNN), and Unet are validated. Regarding dice score, silhouette score, Normalized Mean Squared Error (NMSE), and Root Mean Squared Error (RMSE), the proposed EZWS achieved 0.9723, 0.9847, 0.12, and 0.001; while, the existing algorithms obtained 0.6865, 0.704, 0.545, and 0.015, respectively. Thus, the proposed method had better results with fewer errors.

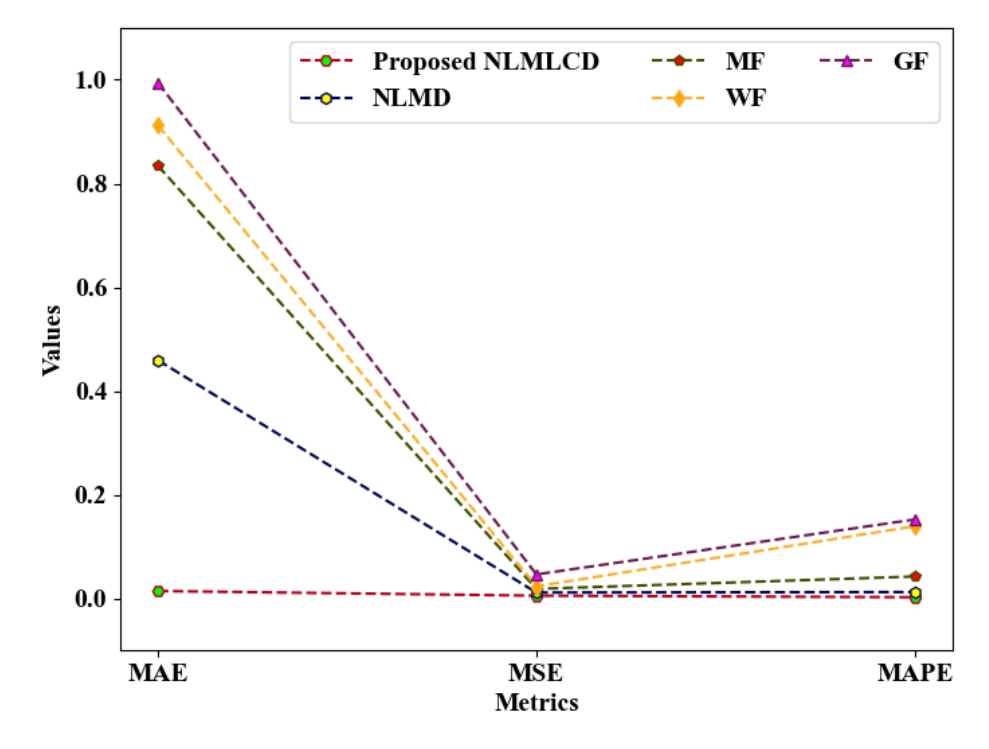


Figure 7: Performance assessment for noise reduction

2025, 10 (44s) e-ISSN:2468-4376 https://jisem-journal.com/

The performance analysis of the proposed NLMLCD and the prevailing algorithms like NLMD, Median Filter (MF), Wiener Filter (WF), and Gaussian Filter (GF) are validated in Figure 7. Regarding Mean Absolute Error (MAE), Mean Squared Error (MSE), and Mean Absolute Percentage Error (MAPE), the proposed NLMLCD achieved 0.014, 0.005, and 0.002; while, the existing methods had overfitting issues. Therefore, the proposed method had higher supremacy.

6. DISCUSSION

Here, a robust MER-DS-EfficientNet and EZWS-based vein-related symptom analysis and multi-PLDD is proposed. The proposed method considered the VS named VER, thus enhancing the disease detection outcomes. Besides, the proposed MER-DS-EfficientNet proficiently classified the numerous categories of PLDs for rice, wheat, maize, and sorghum. Furthermore, key choices like CCA and DHM generation helped to improve the model's superiority. Therefore, the proposed approach obtained accuracy and MSE of 98.9985% and 0.005, respectively. Thus, the harvest and yield quality is improved by the proposed method. Nevertheless, the proposed work heavily focused on PLDD.

Future Scope

This work will focus on climate impact analysis in the future, where the environmental factors (temperature and soil conditions) are considered to enhance the model's efficacy.

7. REFRENCES

- [1] Rice https://www.kaggle.com/datasets/vbookshelf/rice-leaf-diseases
- [2] Wheat https://www.kaggle.com/datasets/olyadgetch/wheat-leaf-dataset
- [3] Maize https://www.kaggle.com/datasets/smaranjitghose/corn-or-maize-leaf-disease-dataset
- [4] Sorghum https://www.kaggle.com/datasets/rogfsdafdsafdsa/sorghum
- [5] Aggarwal, M., Khullar, V., Goyal, N., Singh, A., Tolba, A., Thompson, E. B., & Kumar, S. (2023). Pre-Trained Deep Neural Network-Based Features Selection Supported Machine Learning for Rice Leaf Disease Classification. *Agriculture*, 13(5), 1–24. https://doi.org/10.3390/agriculture13050936
- [6] Ahad, T., Li, Y., Song, B., & Bhuiyan, T. (2023). Comparison of CNN-based deep learning architectures for rice diseases classification. *Artificial Intelligence in Agriculture*, 9, 1–14. https://doi.org/10.1016/j.aiia.2023.07.001
- [7] Alharbi, A., Khan, M. U. G., & Tayyaba, B. (2023). Wheat Disease Classification Using Continual Learning. *IEEE Access*, 11, 1–11. https://doi.org/10.1109/ACCESS.2023.3304358
- [8] Bi, C., Xu, S., Hu, N., Zhang, S., Zhu, Z., & Yu, H. (2023). Identification Method of Corn Leaf Disease Based on Improved Mobilenetv3 Model. *Agronomy*, 13(2), 1–17. https://doi.org/10.3390/agronomy13020300
- [9] Fraiwan, M., Faouri, E., & Khasawneh, N. (2022). Classification of Corn Diseases from Leaf Images Using Deep Transfer Learning. *Plants*, 11(20), 1–14. https://doi.org/10.3390/plants11202668
- [10] Gonzalez, E. M., Zarei, A., Calleja, S., Christenson, C., Rozzi, B., Demieville, J., Hu, J., Eveland, A. L., Dilkes, B., Barnard, K., Lyons, E., & Pauli, D. (2024). Quantifying leaf symptoms of sorghum charcoal rot in images of field-grown plants using deep neural networks. *Plant Phenome Journal*, 7(1), 1–18. https://doi.org/10.1002/ppj2.20110
- [11] Jiang, J., Liu, H., Zhao, C., He, C., Ma, J., Cheng, T., Zhu, Y., Cao, W., & Yao, X. (2022). Evaluation of Diverse Convolutional Neural Networks and Training Strategies for Wheat Leaf Disease Identification with Field-Acquired Photographs. *Remote Sensing*, 14(14), 1–15. https://doi.org/10.3390/rs14143446

2025, 10 (44s) e-ISSN:2468-4376 https://jisem-journal.com/

- [12] Jiang, Z., Dong, Z., Jiang, W., & Yang, Y. (2021). Recognition of rice leaf diseases and wheat leaf diseases based on multi-task deep transfer learning. *Computers and Electronics in Agriculture*, 186, 1–9. https://doi.org/10.1016/j.compag.2021.106184
- [13] Joseph, D. S., Pawar, P. M., & Chakradeo, K. (2024). Real-Time Plant Disease Dataset Development and Detection of Plant Disease Using Deep Learning. *IEEE Access*, 12, 1–24. https://doi.org/10.1109/ACCESS.2024.3358333
- [14] Khan, H., Haq, I. U., Munsif, M., Mustaqeem, Khan, S. U., & Lee, M. Y. (2022). Automated Wheat Diseases Classification Framework Using Advanced Machine Learning Technique. *Agriculture*, 12(8), 1–20. https://doi.org/10.3390/agriculture12081226
- [15] Krishnamoorthy, N., Narasimha Prasad, L. V., Pavan Kumar, C. S., Subedi, B., Abraha, H. B., & Sathishkumar, V. E. (2021). Rice leaf diseases prediction using deep neural networks with transfer learning. *Environmental Research*, 198, 1–8. https://doi.org/10.1016/j.envres.2021.111275
- [16] Kundu, N., Rani, G., Dhaka, V. S., Gupta, K., Nayaka, S. C., Vocaturo, E., & Zumpano, E. (2022). Disease detection, severity prediction, and crop loss estimation in MaizeCrop using deep learning. *Artificial Intelligence in Agriculture*, 6, 1–16. https://doi.org/10.1016/j.aiia.2022.11.002
- [17] Latif, G., Abdelhamid, S. E., Mallouhy, R. E., Alghazo, J., & Kazimi, Z. A. (2022). Deep Learning Utilization in Agriculture: Detection of Rice Plant Diseases Using an Improved CNN Model. *Plants*, 11(17), 1–17. https://doi.org/10.3390/plants11172230
- [18] Li, Y., Sun, S., Zhang, C., Yang, G., & Ye, Q. (2022). One-Stage Disease Detection Method for Maize Leaf Based on Multi-Scale Feature Fusion. *Applied Sciences*, 12(16), 1–19. https://doi.org/10.3390/app12167960
- [19] Lu, Y., Wu, X., Liu, P., Li, H., & Liu, W. (2023). Rice disease identification method based on improved CNN-BiGRU. *Artificial Intelligence in Agriculture*, 9, 1–10. https://doi.org/10.1016/j.aiia.2023.08.005
- [20] Ma, L., Yu, Q., Yu, H., & Zhang, J. (2023). Maize Leaf Disease Identification Based on YOLOv5n Algorithm Incorporating Attention Mechanism. *Agronomy*, 13(2), 1–17. https://doi.org/10.3390/agronomy13020521
- [21] Masood, M., Nawaz, M., Nazir, T., Javed, A., Alkanhel, R., Elmannai, H., Dhahbi, S., & Bourouis, S. (2023). MaizeNet: A Deep Learning Approach for Effective Recognition of Maize Plant Leaf Diseases. *IEEE Access*, 11, 1–15. https://doi.org/10.1109/ACCESS.2023.3280260
- [22] Singh, S. P., Pritamdas, K., Devi, K. J., & Devi, S. D. (2023). Custom Convolutional Neural Network for Detection and Classification of Rice Plant Diseases. *Procedia Computer Science*, 218, 1–15. https://doi.org/10.1016/j.procs.2023.01.179
- [23] Tanveer, M. U., Munir, K., Raza, A., Abualigah, L., Garay, H., Gonzalez, L. E. P., & Ashraf, I. (2024). Novel Transfer Learning Approach for Detecting Infected and Healthy Maize Crop Using Leaf Images. *Food Science and Nutrition*, 13(1), 1–12. https://doi.org/10.1002/fsn3.4655
- [24] Wen, X., Zeng, M., Chen, J., Maimaiti, M., & Liu, Q. (2023). Recognition of Wheat Leaf Diseases Using Lightweight Convolutional Neural Networks against Complex Backgrounds. *Life*, 13(11), 1–22. https://doi.org/10.3390/life13112125